Probing potential energy surfaces with high-resolution spectroscopy

From the Universe's carbon locker to molecular machines

Maltseva, E.O.

Publication date
2017

Document Version
Other version

License
Other

CHAPTER 6

High-resolution gas-phase spectroscopy of a single-bond axle rotary motor

Abstract

High-resolution laser spectroscopy in combination with molecular beams and mass-spectrometry has been applied to study samples of a prototypical rotary motor. Vibrationally well-resolved excitation spectra have been recorded that are assigned, however, to a structural isomer of the original rotary motor which is formed in situ under the elevated temperatures required experimentally. In this isomer the "rotor" and "stator" parts are to a large extent conjugationally disconnected leading to excited-state properties that are dominantly determined by the "rotor" with the "stator" acting as observer.*

*This chapter is adopted from E. Maltseva, S. Amirjalayer, A. Cnossen, W. R. Browne, B. L. Feringa, W. J. Buma.
Tetrahedron, doi.org/10.1016/j.tet.2017.05.064, 2017.

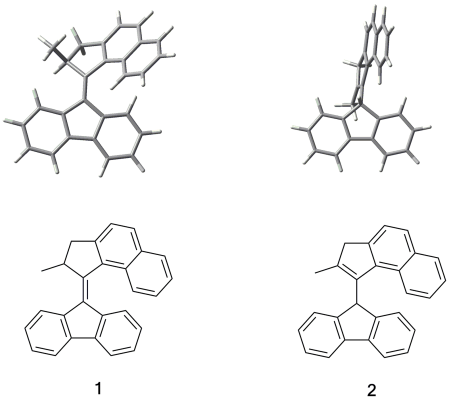

Figure 6.1: Chemical structure of molecular rotor **1** and its isomer **2**.

6.1 Introduction

Inspired by nature, current technology is increasingly aiming for motion that can be controlled at the molecular level. Artificial molecular machines thus nowadays attract tremendous interest as they offer the potential for such a control. Although in many aspects still in its infancy, the field has in recent years matured quickly leading to applications that range from light-controlled catalysis [1–4] to functionalization of surfaces [5,6] and various nanotools in medicine. [7–10]

Rotary motors based on overcrowded alkenes have in this respect shown to be particularly attractive because their properties can be tuned and controlled relatively easily and because light can be used to address them in a non-invasive manner. [11–14] Such rotary motors consist of a "rotor" and "stator" part that are linked by a double bond "axle". Activation of these motors occurs by photoexcitation which initiates a cis-trans isomerization of the "axle". Since this step effectively provides the "power stroke" for the further mechanical motion, it has attracted considerable attention from both experimentalists [15,16] and theoreticians. [17–19] Femtosecond time-resolved fluorescence studies on **1** (Figure 6.1) have found that photoexcitation of the motor is followed by ultrafast (100 fs) relaxation from the Franck-Condon region of the electronically excited "bright" state to a "dark" state that decays on a ps time scale. In these studies it was put forward that this "dark" state is associated with a region of the potential energy surface of the "bright" state with a low oscillator strength, a suggestion that was later supported by computational studies. [20]

Such a two-state isomerization mechanism could, however, not be reconciled from data obtained in subsequent femtosecond time-resolved IR absorption studies on the same system. [21] These studies indicated that the initially excited "bright" state undergoes an ultrafast internal conversion process to a different electronically excited "dark" state that for vertical excitation is quasi-degenerate with the "bright" state but crosses it when the molecule starts to structurally relax on the potential energy surface of the "bright" state. Calculations predict that in this "dark" state the molecule has to overcome a barrier to access the conical intersection with the ground state that leads to isomerization. This three-state model found further support in CASSCF and CASPT2 calculations–the most advanced calculations possible at this moment for such molecular motors–on a slightly

smaller rotary motor.[17]

In view of the above it is clear that a further characterization and understanding of the potential energy surfaces of the lower electronically excited states of **1** is of considerable interest. Ideally, such studies would be performed under conditions in which the molecule is isolated and not affected by its environment. Normally, one would tend to think that such studies need a time-domain approach using femtosecond laser spectroscopic techniques. However, we have shown recently in nanosecond laser spectroscopic studies on the isomerization mechanism of isolated trans-azobenzene[22] that frequency-domain studies can provide a direct–and in some aspects even more detailed–view on the photophysics and photochemistry of electronically excited states with lifetimes down to 170 fs. In the present studies we therefore aimed to apply these high-resolution nanosecond techniques together with supersonic molecular beams and mass-spectrometry on samples of **1** in order to perform mass-selective vibrationally-resolved spectroscopy of this rotary motor. It will be shown that such spectra can indeed be recorded, but further consideration of the observed spectroscopic properties and excited-state dynamics lead to the conclusion that these spectra must be assigned to an isomer of **1** in which "rotor" and "stator" are only connected by a single-bond "axle" (isomer **2**, Figure 6.1).

6.2 Experimental and theoretical details

The molecular beam set up and the employed laser systems have been described in detail before.[23] Here, we will therefore only highlight details that are of direct relevance for the present experiments. In order to create a pulsed molecular beam the sample was heated in a quartz container directly attached to the pulsed nozzle (General Valve) to 180-200° C, slightly higher than its melting point. Expansion into a vacuum with 2 bar Ar using typical opening times of the valve of 200 μs then led to supersonic cooling of the sample molecules. The excited state manifold of these molecules was probed by (1+1') Resonance Enhanced Two-Photon Ionization (RE2PI) spectroscopy in combination with mass-resolved ion detection. In these experiments excitation of the molecule in the wavelength range of 330-355 nm with a laser-limited resolution of less than 0.1 cm^{-1} was provided by the second harmonic of a Cobra-Stretch dye laser while an ArF excimer laser (Neweks PSX-501, 193 nm) was used for subsequent ionization. Ions generated in this way were detected using a reflectron type time-of-flight mass spectrometer (R.M. Jordon D-850). Typical excitation and ionization pulse energies were 0.1-0.2 and 2 mJ, respectively. Excitation spectra have been recorded using excitation and ionization laser pulses that were overlapped in time, while for pump-probe experiments the delay between these two lasers was scanned using a delay generator (Stanford Research DG-535). To compare the experimental results with theoretical predictions, (Time Dependent) Density Functional Theory (TD-DFT) calculations have been performed with the Gaussian09 version E01[24] suite of programs on the equilibrium geometries and harmonic force fields of ground and electronically excited states of the rotary motor, its single-bond axle derivative, and several components of these molecular systems. Although various basis sets and functionals have been explored, we report here the result of calculations at the 6-31G*/B3LYP level.[25–27] The same suite of programs has been used as well for simulating vibrationally-resolved excitation spectra at the FranckCondon (FC) levels of approximation[28,29] using a scaling factor for the vibrational frequencies of 0.96.[30] Compound **1** was available from earlier studies.[11]

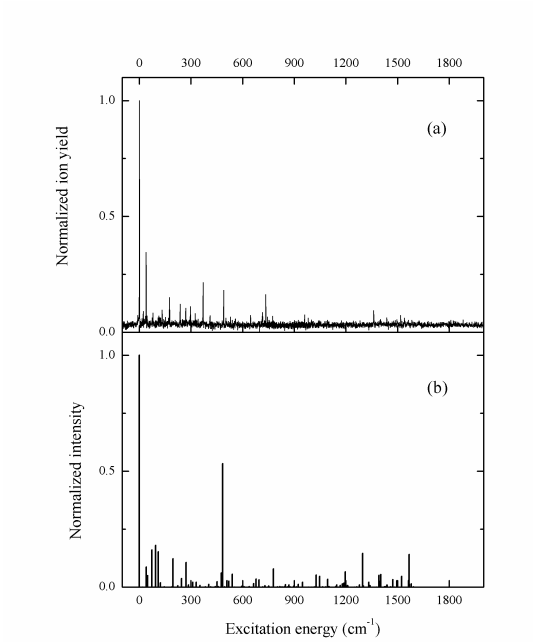

Figure 6.2: (a) (1+1') RE2PI excitation spectrum taken at molecular mass; (b) $S_1 \leftarrow S_0$ simulated fundamental excitation spectrum of **2** excluding modes at 20 and 85 cm^{-1}. Excitation energies are given with respect to the 0-0 transition at 28618.8 cm^{-1}.

6.3 Results and Discussion

Figure 6.2(a) displays the (1+1') RE2PI excitation spectrum of the sample detected at m/e = 344 a.m.e., the mass of the molecular ion, and recorded in the 28500-30800 cm^{-1} (351-325 nm) frequency region. The spectrum shows well-separated bands with a line width between 1.1 and 1.5 cm^{-1}. Outside this region no other bands have been detected. The lowest-energy band in this spectrum occurs at 28618.8 cm^{-1}. Since at lower excitation energies no other bands are observed we assign this band as the 0-0 transition to the lowest electronically excited state. Interestingly, the vibronic activity in this spectrum is rather limited: apart from the strong 0-0 transition only a few low-intensity bands are present at higher excitation energies (Figure 6.2(a)). Quantum chemical calculations on **1** predict that for vertical excitation the lower two electronically excited states are quasi degenerate.[21] One of these two states has a large oscillator strength, while the other one has an oscillator strength that is three orders of magnitude smaller. Importantly, these calculations do not find a stable energy minimum on the potential energy surface of the "bright" state, but for the "dark" state such a minimum is found without problem. One would thus in first instance be inclined to assign the excitation spectrum to the excitation spectrum of the "dark" state.

The wavelength at which the 0-0 transition is detected (349.4 nm) is in that case,

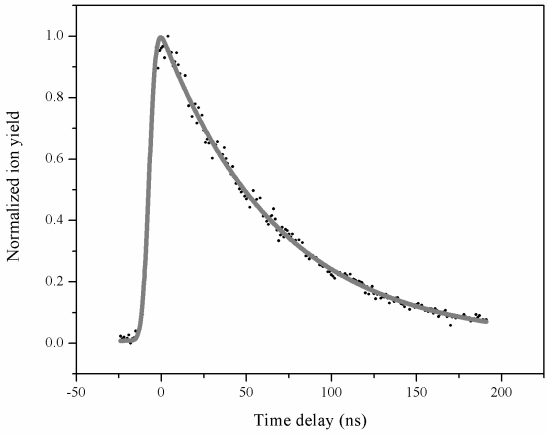

Figure 6.3: Time-delay trace of (1+1') RE2PI signal at 0-0 transition.

however, quite puzzling since the absorption spectrum of **1** dissolved in d-cyclohexane shows a band associated with absorption by the "bright" state that has a maximum at 390 nm and extends to 440 nm.[21] Assignment of the spectrum in Figure 6.2(a) to the "dark" state would imply that the "bright" state is at shorter wavelengths than 350 nm. Although a blue shift of the absorption spectrum upon going from solution to the gas phase is quite normal, the magnitude of the shift observed here falls outside the range one would expect. A scenario that theoretically might lead to such a large shift is that the molecule adopts a significantly different geometry–in particular with respect to the dihedral angle between the rotor and the stator part–under solution and gas-phase conditions. However, such an explanation is not supported by recent high-resolution rotational spectroscopic experiments on **1**[31] which for all practical purposes show that in the gas phase the "rotor" and "stator" adopt the same relative orientation as determined previously with X-ray crystallography.[32]

For the further assignment of the excitation spectrum in Figure 6.2 it is instructive to consider the absorption spectra of the isolated stator and rotor moieties. The "stator" is then a simple fluorene entity that has its absorption maximum around 300 nm[33] in solution and its 0-0 transition at 296.0 nm in supersonic expansions.[34] The "rotor" part, on the other hand, is an alkyl-substituted naphthalene with an absorption maximum around 315-320 nm.[35] In the rotary motor an extended conjugated system is present. If "stator" and "rotor" would be perpendicular, the absorption spectrum of the motor is expected to be the superposition of the absorption spectra of the isolated parts. Conjugation, on the other hand, red-shifts the absorption maximum but the amount to which this red shift occurs will depend on the degree to which conjugation is extended.

To study in more detail the dynamics of the electronic state that is excited in our experiments we have performed pump-probe RE2PI experiments in which the ion yield at the molecular mass is monitored as a function of the delay between excitation and

ionization laser pulses. Figure 6.3 shows the decay trace that is obtained after excitation of the 0-0 transition at 28618.8 cm^{-1}. This trace can be well fitted by the convolution of the instrument response associated with the convolution of the two laser beams (represented by a Gaussian function with a width of 8 ns) and a mono-exponential decay with a time constant of (68.5±0.8) ns. It is important to emphasize that our experimental setup allows for indirect detection of excited states with lifetimes even down to 170 fs in which case the pump-probe trace merely shows the convolution of the excitation and ionization lasers.[22] Similarly, it is also important to realize that quite a different decay trace is expected if the excited state would first decay within our time resolution to another excited state with a longer lifetime that is then ionized. In that case the decay trace would display the instrument response followed by an exponential decay with a reduced amplitude.[36] The measured decay traces thus demonstrate that in our experiments decay is observed of the same electronic state that has been excited.

Small signal intensities preclude similar pump-probe experiments at higher excitation energies. Nevertheless, the fact that significant broadening of bands at higher excitation energies is not observed indicates that there is no strong dependence of the lifetime on the excitation energy. There is thus no indication for the onset of additional decay channels as is observed, for example, in molecular-beam spectra of azobenzene[22] and as has been predicted in theoretical studies on the "dark" state of **1** that find that at the equilibrium geometry of the "dark" state of **1** the molecule needs to overcome a barrier in order to access the conical intersection with the ground state.[21]

The spectroscopic properties and excited-state dynamics that emerge from our experiments thus indicate that the excitation spectrum displayed in Figure 6.2(a) is not associated with **1**. However, since the spectrum is detected at the molecular mass of **1** and clearly concerns molecules that are supersonically cooled, we have to conclude that it derives from another isomer of **1** that is made in situ under our elevated temperature conditions. The discussion on the spectroscopy of the "rotor" and the "stator" (*vide supra*) leads to the conclusion that in this isomer the relevant chromophore is most likely a modified "rotor" part with an extended conjugation. Consideration of possible isomers expected to have the spectroscopic and dynamical properties as observed in our experiments but at the same time also not requiring extensive reaction pathways suggest that isomer **2** might very well be the absorbing species in Figure 6.2(a). The isomerization reaction from **1** to **2** entails a formal 1,3-hydrogen shift which is symmetry allowed as a thermal, antarafacial shift, but in practice prohibited by structural demands. Calculations that we performed on this reaction indeed find a barrier of 78 kcal/mol. At the same time it is well known that the reaction is easily catalyzed with an acid or base catalyst.[37]

Quantum chemical calculations on the ground state of **1** and **2** show that the two isomers differ by about 1 kcal/mol in energy, **1** being the more stable isomer. From a thermodynamic point of view it is therefore very likely that at 180-200° C a significant fraction of **2** is present. Interestingly, we find that in **2** the "rotor" part becomes completely planar (Figure 6.1)–thus optimizing conjugation with the naphthalene moiety–while in **1** the non-aromatic five-membered ring is non-planar. Also, in **1** the aromatic planes of the "stator" and the "rotor" make an angle close to 50°,[31] but in **2** steric repulsions and the relieve of conjugation requirements between "stator" and "rotor" lead to a structure in which the two parts are nearly perpendicular to each other (Figure 6.1). TD-DFT calculations show that the first electronically excited state is associated with the strongly allowed HOMO → LUMO excitation (f=0.16 for vertical excitation) localized on the "rotor" part. The calculations predict that the 0-0 transition occurs at 3.43 eV (372 nm) which, in view of the level of the calculations, agrees nicely with the experimentally ob-

served value of 3.55 eV (349 nm). The fact that the calculations predict a slightly lower adiabatic excitation energy can to a large part be traced back to a minor mixing in of the HOMO-1 $\rightarrow$ LUMO excitation which is effectively a charge-transfer excitation since the HOMO-1 orbital is localized on the "stator" part. As DFT calculations are well known to underestimate the excitation energies of charge transfer excitations, such mixing will lead to an underestimation of the excitation energy of S_1 of **2**.

Further support for the conclusion that **2** is the carrier of the excitation spectrum is provided by simulations of the vibronic activity in the $S_1 \leftarrow S_0$ excitation spectrum of **2**. Calculations at the Franck-Condon level give in first instance rise to a spectrum in which extensive progressions are present of two low-frequency modes that dominantly involve motions of the "rotor" and "stator" parts with respect to each other. A priori it is to be expected that at the present level of calculation it will be quite difficult to calculate their activity, in particular also because the previously mentioned mixing in of charge transfer character into S_1 will give rise to displacements along such inter-component coordinates that in reality are absent. Figure 6.2(b) therefore displays a stick spectrum in which the intensities of all v^1_{i0} transitions are plotted except for the two aforementioned low-frequency modes. Overall a reasonable agreement is observed between experiment and theory, albeit that the 0-0+490 cm^{-1} band is predicted to have a considerably greater intensity than observed experimentally.

Finally, we note that our calculations on **2** predict a radiative lifetime that is close to the experimentally observed decay time of the REMPI signal. We thus can conclude that internal conversion to the ground state is relatively slow as would be expected on the basis of the energy gap between the two states and the absence of conical intersections. It is also in agreement with what one would expect from the nonradiative decay properties of (substituted) naphthalenes.

Above we have discussed the excitation spectrum that is observed in the 351-325 nm region and that has been assigned to isomer **2**. In our experiments we have actually scanned a much larger wavelength region (350-470 nm) but using mass-resolved ion detection at the mass of the molecular ion have not observed any other band system that might originate from isomer **1**. This does not mean that isomer **1** is not present in the supersonic expansion. In fact, ref. 31 reports on rotational spectroscopic studies on **1** that use for all practical purposes the same experimental conditions as in the present study. From these observations we conclude that the electronically excited states of **1** under isolated conditions are subject to extremely fast internal conversion which prohibits their observation in nanosecond REMPI experiments. In view of these ultrafast dynamics it would be highly interesting to perform REMPI experiments with picosecond lasers. In such experiments much higher photon fluxes are available that might make the ionization channel become competitive with the internal conversion channel while still retaining a useful spectral resolution.

6.4 Conclusions

In the present study two-color RE2PI laser spectroscopic techniques in combination with molecular beams have been applied on samples of a well-known rotary motor. Mass-resolved ion detection at the mass of the molecular ion has led to the observation of a vibrationally well-resolved excitation spectrum with narrow bands that do not carry signatures of lifetime broadening. Consideration of the spectroscopic and excited-state dynamics characteristics of this spectrum have been shown to lead to the conclusion

that the spectrum cannot originate from rotary motor **1** but must derive from one of its isomers. In combination with quantum chemical calculations it has been shown that isomer **2**, in which "rotor" and "stator" are connected with a single-bond "axle" instead of a double bond, nicely fits the experimental observations.

References

1. S. F. Pizzolato, B. S. L. Collins, T. van Leeuwen, B. L. Feringa. *Chem. A Eur. J.*, **23**, 1, 2017.
2. R. Göstl, A. Senf, S. Hecht. *Chem. Soc. Rev.*, **43**, 1982, 2014.
3. V. Blanco, D. A. Leigh, V. Marcos. *Chem. Soc. Rev.*, **44**, 5341, 2015.
4. R. S. Stoll, S. Hecht. *Angew. Chem., Int. Ed.*, **49**, 5054, 2010.
5. J. Vachon, G. T. Carroll, M. M. Pollard, E. M. Mes, A. M. Brouwer, B. L. Feringa. *Photochem. Photobiol. Sci.*, **13**, 241, 2014.
6. K.-Y. Chen, O. Ivashenko, G. T. Carroll, J. Robertus, J. C. M. Kistemaker, G. London, W. R. Browne, P. Rudolf, B. L. Feringa. *J. Am. Chem. Soc.*, **136**, 3219, 2014.
7. S. Balasubramanian, D. Kagan, C.-M. J. Hu, S. Campuzano, M. J. Lobo-Castañon, N. Lim, D. Y. Kang, M. Zimmerman, L. Zhang, J. Wang. *Angew. Chem., Int. Ed.*, **50**, 4161, 2011.
8. M. M. Lerch, M. J. Hansen, G. M. van Dam, W. Szymanski, B. L. Feringa. *Angew. Chem., Int. Ed.*, **55**, 10978, 2016.
9. H. Peng, X.-F. Li, H. Zhang, X. C. Le. *Nat. Commun.*, **8**, 14378, 2017.
10. R. Klajn, J. F. Stoddart, B. A. Grzybowski. *Chem. Soc. Rev.*, **39**, 2203, 2010.
11. J. Conyard, K. Addison, I. A. Heisler, A. Cnossen, W. R. Browne, B. L. Feringa, S. R. Meech. *Nat. Chem.*, **4**, 547, 2012.
12. B. L. Feringa. *Acc. Chem. Res.*, **34**, 504, 2001.
13. N. Koumura, E. M. Geertsema, M. B. van Gelder, A. Meetsma, B. L. Feringa. *J. Am. Chem. Soc.*, **124**, 5037, 2002.
14. R. A. van Delden, M. K. J. ter Wiel, M. M. Pollard, J. Vicario, N. Koumura, B. L. Feringa. *Nature*, **437**, 1337, 2005.
15. J. Conyard, A. Cnossen, W. R. Browne, B. L. Feringa, S. R. Meech. *J. Am. Chem. Soc.*, **136**, 9692, 2014.
16. R. Augulis, M. Klok, B. L. Feringa, P. H. M. van Loosdrecht. *Phys. Status Solidi C*, **6**, 181, 2009.
17. F. Liu, K. Morokuma. *J. Am. Chem. Soc.*, **134**, 4864, 2012.
18. M. Filatov. *Wiley Interdiscip. Rev.: Comput. Mol. Sci.*, **3**, 427, 2013.
19. A. Nikiforov, J. A. Gamez, W. Thiel, M. Filatov. *J. Phys. Chem. Lett.*, **7**, 105, 2016.
20. X. Pang, X. Cui, D. Hu, C. Jiang, D. Zhao, Z. Lan, F. Li. *J. Phys. Chem. A*, **121**, 1240, 2017.
21. S. Amirjalayer, A. Cnossen, W. R. Browne, B. L. Feringa, W. J. Buma, S. Woutersen. *J. Phys. Chem. A*, **120**, 8606, 2016.
22. E. M. M. Tan, S. Amirjalayer, S. Smolarek, A. Vdovin, F. Zerbetto, W. J. Buma. *Nat. Commun.*, **6**, 5860, 2015.
23. S. Smolarek, A. Vdovin, A. Rijs, C. A. van Walree, M. Z. Zgierski, W. J. Buma. *J. Phys. Chem. A*, **115**, 9399, 2011.
24. M. J. Frisch, G. W. Trucks, H. B. Schlegel, G. E. Scuseria, M. A. Robb, J. R. Cheeseman, G. Scalmani, V. Barone, B. Mennucci, et al. *Gaussian 09, Revision E. 01; Gaussian.* 2009.
25. G. A. Petersson, A. Bennett, T. G. Tensfeldt, M. A. Al-Laham, W. A. Shirley, J.

Mantzaris. *J. Chem. Phys.*, **89**, 2193, 1988.
26. A. D. Becke. *Phys. Rev. A*, **38**, 3098, 1988.
27. C. Lee, W. Yang, R. G. Parr. *Phys. Rev. B*, **37**, 785, 1988.
28. T. E. Sharp, H. M. Rosenstock. *J. Chem. Phys.*, **41**, 3453, 1964.
29. E. V. Doktorov, I. A. Malkin, V. I. Man'ko. *J. Mol. Spectrosc.*, **64**, 302, 1977.
30. I. M. Alecu, J. Zheng, Y. Zhao, D. G. Truhlar. *J. Chem. Theory Comput.*, **6**, 2872, 2010.
31. S. R. Domingos, A. Cnossen, W. J. Buma, W. R. Browne, B. L. Feringa, M. Schnell. *Angew. Chem. Int. Ed.*, in press, 2017.
32. J. Vicario, A. Meetsma, B. L. Feringa. *Chem. Commun.*, **116**, 5910, 2005.
33. M. Ramart-Lucas, M. J. Matti, T. Guilmart. *Bull. Soc. Chim. Fr.*, **15**, 1215, 1948.
34. B. H. Boo, J. K. Lee. *J. Korean Phys. Soc.*, **60**, 496, 2012.
35. N. G. Adams, D. M. Richardson. *Anal. Chem*, **23**, 129, 1951.
36. E. Maltseva, S. Amirjalayer, W. J. Buma. *Phys. Chem. Chem. Phys.*, **19**, 5861, 2017.
37. H. Logtenberg, J. Areephong, J. Bauer, A. Meetsma, B. L. Feringa, W. R. Browne. *ChemPhysChem*, **17**, 1895, 2016.